Intracochlear Recordings of Electrophysiologic Parameters Indicating Cochlear Damage

Oliver F. Adunka, MD, **Stefan Mlot, BA**, **Thomas A. Suberman, BA**, **Adam P. Campbell, BA**, **Joshua Surowitz, MD**, **Craig A. Buchman, MD**, and **Douglas C. Fitzpatrick, PhD**
Department of Otolaryngology/Head and Neck Surgery, University of North Carolina at Chapel Hill, Chapel Hill, NC, USA

Abstract

Objective—The pathophysiologic mechanisms resulting in hearing loss during electrode implantation are largely unknown. To better understand the functional implications of electrode implantation, we recorded the effects of cochlear damage on acoustically evoked intracochlear measurements using normal-hearing gerbils.

Methods—A metal electrode was placed on the surface of the round window and recordings of the cochlear microphonic (CM) and compound action potential (CAP) were made in response to stimulation with tone bursts at various frequencies in one-octave intervals and at intensities of 15-72 dB SPL. The electrode was then advanced incrementally, with CM and CAP measurements taken at each step. These data were compared to data taken at the round window, and the electrode was withdrawn when a significant change was observed. Following electrophysiological analysis, the cochlea was examined histologically.

Results—Results show that upon electrode insertion, loss of amplitude in the CM and CAP occurs after damage to cochlear structures. Loss of activity was typically first apparent in the CAP rather than the CM.

Conclusions—These results suggest that a reduction of the CAP can be an early marker of interaction of the electrode with cochlear structures. Such measurements are potentially available with slight modifications to current cochlear implant technology.

INTRODUCTION

The ipsilateral combination of electric and acoustic hearing (also termed electric-acoustic stimulation; EAS[1,2], hybrid stimulation, or partial deafness cochlear implantation; PDCI[3]) has been shown to improve speech recognition scores. Unfortunately, in most patients, residual hearing is at least partially compromised during implantation[4-6]. Prior human temporal bone experiments have helped to elucidate trauma mechanisms of intracochlear electrode placement[7-12]. These studies have helped to optimize surgical cochleostomy placement[13,14]. Also, several efforts have lead to improved cochlear implant electrode designs facilitating atraumatic insertions, which seem critical for hearing preservation[8,15]. Also, recent clinical research suggests the importance of atraumatic electrode placement not

only for hearing conservation but also in standard cochlear implantation in the profoundly hearing impaired ear[16,17].

Despite these advances, the exact factors for the success or failure of hearing preservation remain enigmatic. Since human experiments are limited, an animal model can help to shed light on these factors. Consequently, we have begun development of a gerbil model to identify electrophysiological markers of cochlear damage. Ultimately, the goal is to identify physiological markers that can be used intraoperatively to detect intracochlear trauma and electrode positioning. As a first step toward this goal, we evaluated the effects of cochlear damage on intracochlear measurements of acoustically evoked potentials including the cochlear microphonic (CM) and compound action potential (CAP) in normal hearing animals. Ultimately, these results will be useful to provide a scientific base to interpret physiological feedback on the structural and functional integrity of the cochlea during the electrode insertion process.

METHODS

Results from 10 ears in 9 Mongolian gerbils are reported. The gerbil was chosen for the animal model because it has good low frequency hearing and the cochlea is readily accessible. Low frequency hearing is important because our ultimate aim is to preserve low frequency hearing during human cochlear implantation. All animals were handled using protocols approved by the local IACUC.

Animal handling

Surgeries and recordings were performed under deep urethane anesthesia (25% solution in saline, 1.5 g/kg, i.p.). Once anesthesia was induced, the animal was moved to a double-walled, sound attenuated booth for the remainder of the experiment (up to 10 hours). Body core temperature and heart rate were monitored. Serial numbering was not consecutive as concurrent experiments were performed.

Surgical Procedure

After anesthesia was induced, superficial tissues were dissected, the pinna was removed, and the bone of the bulla was identified. The bony bulla was opened and the round window niche, the spiral modiolar artery, and all other structures of the bulla were identified. Once the round window was visible within its niche, an intracochlear recording electrode, which was attached to a micromanipulator, was positioned and placed onto the membrane.

Acoustic Stimulation & Calibration

The stimuli were tone bursts with a 10 ms plateau and 2 ms rise/fall times, and a 30 ms interstimulus interval. Electrical signals were generated and delivered to a well-shielded loudspeaker (Beyer DT-48) using custom software, a National Instruments input/output board (model 6250E), and a Tucker-Davis system III headphone buffer (model HB7). The speaker was 15 cm from the animal's tympanic membrane. The speaker output was delivered through a small plastic tube that could be crimped to reduce sound output independent of the electrical signal delivered to the speaker as a test for shielding against electrical artifact. Calibration was performed using a ¼" Bruel and Kjaer microphone placed at the position of the animals eardrum, and levels were presented in dB SPL (re 20 μPal).

Electrode & Recording Configuration

The electrode used was a 50 μm diameter, Teflon-insulated tungsten-iridium wire with about 50 μm of tip insulation removed. This size was appropriate relative to the gerbil scala tympani, which typically ranges from a diameter of about 700 μm in the basal turn to about

300 μm in higher turns[18]. The electrode was rigid and attached to a hydraulic micromanipulator, which was controlled from outside the sound booth in steps as small as 1 μm. The recording was differential and monopolar, with the electrode connected to the positive input of a preamplifier (Grass Instruments, model P15D), a wire clipped to a neck muscle was connected to the negative input, and the system ground was connected to the animal's tail. Amplification was 100x and filters were bandpass from 300-50,000 Hz. The output led outside the sound booth where there was additional amplification (10x) and filtering (300-100,000 Hz). The waveform was then digitized (200 kHz sampling rate) and 100 stimulus repetitions were averaged.

Intracochlear Recordings

Recording electrode penetrations were made into scala tympani through the round window membrane. Penetrations were intended to be almost perpendicular to the long axis of scala tympani to assure traumatic penetrations of the BM, osseous spiral lamina, and spiral ligament. In the gerbil, the rough positions of these structures are visible through the round window. Specifically, the electrode was directed towards the BM evidenced by a darker shadow within the basal turn. Recordings of the intracochlear potentials to acoustic stimuli were made at intervals as the electrode was advanced.

At each step, an automated stimulation and recording sequence of tone frequencies and intensities was used. The frequencies used were 1, 2, 4, 8, and 16 kHz. At the most sensitive frequencies (typically 4 and/or 8 kHz), levels were from 72-15 dB in 3 dB steps. To isolate the CM and the CAP, digital processing of the averaged waveform was performed with post-filtering. Once an entire series was complete, data across all frequencies were evaluated and observed for changes when compared to the initial recordings taken at the round window.

Assessment of Cochlear Status and Electrode Position

Histology subsequent to each experiment was critical for determining the site and degree of cochlear damage. After each experiment, each animal was sacrificed and the cochlea was removed en block. The whole mounts were decalcified and stained with toluidine blue.

Data collection and analysis

The CM and CAP were separated by appropriate filtering and by analyzing particular epochs of the recorded waveform. The CM signal was analyzed from the last 5 ms of the 10 ms plateau. Its magnitude at the stimulus frequency was determined from the amplitude component of the response. To measure the CAP we analyzed the epoch from 1-6 ms after stimulus onset. The CAP has the approximate shape of an action potential with a duration of ~1 ms, so its major frequency components are near 1000 Hz. We thus filtered from 300-1500 Hz to remove the CM for most stimulus frequencies, and measured the peak-to-peak amplitude over the analysis period.

Thresholds for the CM and CAP were determined by fitting curves through suprathreshold responses and determining when the fitted lines crossed the noise floor (see Figure 2B). The noise floor was measured by analyzing the response in the last 5 ms of the interstimulus period.

In addition to threshold measurements, our data sets consisted of complete "response areas" or responses across a range of frequencies and intensities. Thus, a large number of suprathreshold intensities were compared between responses taken at various locations. These comparisons were made visually from contour plots created in MATLAB from the subtraction of the response within the cochlea (the "test" response) from that taken at the round window (the "standard" response). Statistical comparisons were made using paired t-

tests for responses taken at the same frequency and intensity in the standard and test responses. Only data points that were above threshold in the standard responses were included in the statistical comparisons.

RESULTS

A summary of the cases is shown in Table 1. The table describes the location and degree of damage in each cochlea, the best frequency and minimum threshold of the CM and CAP at the round window, and the magnitude and frequency range of response changes associated with the damage to cochlear structures. The final column identifies cases where there was recovery of function after withdrawal of the electrode.

Anatomical approach

In each case, the electrode was directed radially through the round window toward the basilar membrane (BM). A typical case is shown in Figure 1, where the perforation in the round window and the intracochlear damage are apparent. In this ear, the trauma on the BM included an area from the edge of the osseous spiral lamina (OSL) to the outer hair cells (OHCs). At the site of damage there was a tear in the BM and there was loss of OHCs, indicating mixture of endolymph and perilymph. As measured from the specimen, the distance traversed was about 650 μm. The physiology from this case showed a reduction in cochlear potentials at an insertion depth of 700 μm.

Naturally, the length of the penetration varied with the insertion angle. Damage to the BM was most common, although in some cases damage included the OSL and in one case it was restricted to the OSL (Table 1). In five of the cases a breach between scala tympani and media could be observed with consequent assumed loss of the EP. Cases without an obvious breach were associated with a smaller magnitude of physiological damage, and it was only in a subset of these cases that reversibility was observed.

Recordings at the round window

Physiological results described in the next three figures are from the same case as in Figure 1. A level series of recordings to a 4-kHz signal obtained at the round window is shown in Figure 2. Traces shown in the left column of Figure 2A are the raw averaged time waveforms, where the CM is the fine structure sinusoid that lasts for the duration of the stimulus and the CAP is the lower frequency wave seen near the onset of the stimulus. The traces in the middle column of 2A show the power spectrum of the epoch from 5-10 ms in each recording, which was used to measure the magnitude of the CM. A strong response component at the stimulus frequency of 4 kHz was apparent across a wide range of sound levels. The traces in the right column of 2A show each response after filtering from 0.5-1.5 kHz to isolate the CAP. The peak of the CAP occurred at an increasing latency as the stimulus level was lowered, typical of neural responses to auditory stimuli. All of the curves are normalized to the maximum at that sound level. Because of the normalization the signals appear noisier at lower intensities.

We determined thresholds using the power spectrum of the CM (Figure 2B) and the peak-to-peak magnitude of the CAP (Figure 2B). The noise level was obtained during an epoch with no stimulus present (last 5 ms of the recording duration). A line was fit to the data points and threshold was estimated as the point where the line intersected the noise level. For the CM, the response magnitude decreased linearly over the range of sound levels tested (blue circles). For the CAP, the response magnitude (root mean square power of the epoch from 1-6 ms) was typically saturating, so a logistic function was used for the fit. Using a consistent signal/noise level to determine thresholds for the CM and CAP ensured that their

sensitivity could be meaningfully compared. The sensitivity of the CM in this case (threshold = 13 dB SPL) was greater than that for the CAP (threshold = 21 dB SPL). Greater sensitivity of the CM was a consistent result.

Data for all frequencies used are shown in Figure 2C. The data points for these "response areas" are indicated by black dots, and the responses are displayed as contours interpolated between the points (contour function in MATLAB). The magnitude of response is normalized to the maximum and expressed as dB increments of the color scale. The thresholds across frequencies are indicated by the white lines. For both the CM and CAP, the greatest response magnitude and the lowest thresholds were to 4 kHz. Across ears, either 4 or 8 kHz was the most sensitive frequency, with 4 kHz being more common.

Across all ears, CM thresholds were more sensitive than CAP thresholds, with an average difference of 7.4 dB (range 2.9-9.7 dB for the five frequencies tested). The threshold differences between the CM and CAP were significant (paired t-test, $p < 0.01$) for all frequencies except for the smallest difference, which was at 8,000 Hz. The significance level of $p < 0.01$ corresponds to the 5% level after the Bonferroni correction for tests at five frequencies.

Responses during electrode advancement

Response areas taken at the round window represent the "standard" for each case, and responses taken as the electrode was advanced through the scala tympani were compared to this standard. The comparison was made by subtracting the "test" response at each depth from the standard. Results of the subtraction from two depths of insertion for the case shown in Figures 1 and 2 are shown in Figure 3. In these plots the color scale has been shifted such that a result of zero, or no difference, is indicated by a shade of green. In this way the plot can indicate either an increase or loss compared to that of the standard. For illustrative purpose, a decrease of response is indicated by a shift into the red range and an increase by a shift into the blue range. In Figure 3A, the electrode was at a depth of 250 μm. The threshold curve for the standard is the white line, while that for the test is the red line. At this depth, the test response was on average slightly larger than the standard (shift of color into the blue range). A slight increase in response when the electrode had penetrated the round window was a common result. The recording taken as the electrode impacted the BM, as indicated by the correspondence between this depth (700 μm) and the subsequent histology (Figure 1) is shown in Figure 3B. There was a large loss of response, indicated by a shift into the red range when the impact occurred.

A quantification of the complete track is shown in Figure 3C. The data points represent the percent change in the total response magnitude (i.e., all points above threshold summed) between the test and standard responses. Filled symbols represent points where the difference was significant (paired t-test, $p < 0.05$) and open symbols are points where the difference was not significant. A large loss of response of both the CM and CAP occurred at the depth of 700 μm (contour plot shown in Figure 3B). In this case, when the electrode was retracted from this depth (arrow), recovery of the response did not occur.

The CAP was often the more sensitive measure of cochlear damage

Despite its lower overall sensitivity to the acoustic stimuli compared to the CM, in most cases (6/10) the CAP was the more sensitive physiological marker for interaction with cochlear structures. Results from four of these cases are shown in Figure 4. The data shown are the contour plots at the depth where a significant reduction in the CAP was first obtained (red color range), while the response to the CM was not significantly different from the standard (green color range).

Cases with recovery of response after withdrawal of the electrode

Figure 5 shows that we were able to identify trauma at a reversible stage. The response shown in Figure 5A was the first significant reduction in the CAP, with no significant change in the CM. When the electrode was withdrawn, the CAP response recovered almost completely (Figure 5B, C). The change in the CAP at the depth shown in Figure 5A (700 μm) was small but significant (~5% loss of response), indicating the sensitivity of the technique. No damage was seen histologically in this case. Partial recovery was seen in one additional case, with only slight damage to the OSL visible in subsequent histology (see Figure 6C). These results indicate that electrophysiological measures could provide a sensitive enough marker of imminent damage.

Correlation between magnitudes of physiological and anatomical damage

The magnitude of loss of the physiological responses showed a good correlation to the degree of anatomical damage caused by the electrode. Additional examples of the magnitude and threshold changes in the physiological responses and the attendant anatomical damage are shown in Figure 6.

DISCUSSION

In this report we demonstrate the ability to detect intracochlear damage by measuring acoustically evoked intracochlear potentials in a normal hearing animal model. Our ultimate aim is to translate this methodology into the intraoperative setting as a guide to electrode placement and to aid in the preservation of residual hearing. This study is several steps away from that goal, but describes a "proof of concept" and some early results. Interestingly, the main results were that the CAP in most cases was a more sensitive marker of early interaction between the electrode and cochlear structures than was the CM, and that when detected early enough there could be recovery after electrode retraction and no breach of the cochlear partition.

While previous animal studies from other groups have measured the effects of intracochlear measurements on early auditory potentials such as the CM and the CAP[19-21], the actual recordings were not performed using an electrode positioned within the cochlea. Recordings within the cochlea are expected to be much more sensitive than those recording more remotely. Also, the overall aim of those studies was to document changes in the central auditory system after cochlear injury and the cochlear damage was typically much greater. Hence, despite some similarities, the present report clearly differs in many ways.

The fact that the CAP proved to be a more sensitive marker of intracochlear damage was surprising. One possibility is that the CM when measured by our monopolar recording configuration is summed over a greater proportion of the cochlea than is the CAP, so that the CAP is more sensitive to damage restricted to a single location. That is, assuming the CM represents the output of a larger fraction of the cochlea than does the CAP, then a small, local change would have less effect on the CM than the CAP. This hypothesis can be tested in future experiments by placing the return electrode closer to the active electrode providing for less spatial summation in the responses. Previous experiments to measure local CMs in the gerbil or guinea pig cochlea have used a return electrode located in the scala vestibuli at the same position within the cochlea as the active electrode in the scala tympanie.g.,[22,23]. These authors noted that the recording can be considered truly local only when the potentials at the two electrodes are 180 degrees out of phase, corresponding to the motion of the BM toward each electrode. This recording configuration is not one that would be available clinically. However, a return electrode located on a contact should be possible, and may provide much greater spatial selectivity. Another possibility is that the CAP may be derived

from more basal sections of the cochlear than the CM. If so, the pattern of CAP vs. CM sensitivity to cochlear damage may vary with location and stimulus frequency.

Across and within cases, there was an inconsistency in the affected frequency range. As shown in Figure 4 and Table 1, in some instances the initial effect in the CM was at higher or lower frequencies than the CAP, and across cases the changes could be initially and/or primarily at high, middle or low frequencies. At present we have not identified a clear anatomical correlate for these differences.

Unlike a clinical implant, the electrode used in our experiments was a rigid metal rod. Because of its rigidity, it is more likely than not that the electrode would penetrate rather than bounce off the soft cochlear tissues. We chose this approach to increase our ability to induce trauma. However, we are currently experimenting with modifications of the tip region as well as with more flexible materials in order to better simulate an actual implant electrode. In addition to differences in electrode design, our model also differs from the clinical situation in the state of hearing. The current experiments were performed in normal-hearing animals, because we intended to use the most sensitive preparation to detect the electrophysiologic consequences of damage. Future experiments could employ a more clinically relevant experimental design by using animals with various levels of hearing loss.

An important result in the current experiments is that the change in response during interaction of the electrode and cochlear structures was not seen only near CF and at threshold intensities, but occurred across a wide range of frequencies and intensities. This result means that to detect such interactions it is not necessary to record complete response areas as was done here. Instead, smaller ranges of frequency and intensity would be suitable; in fact, a single frequency and intensity could potentially be used. Because the responses at high intensities are large, relatively few repetitions can produce a consistent averaged response. This is an important practical consideration for the intraoperative use of the techniques. Similar speed and accuracy would be unlikely to be obtained if the measurements were not intracochlear, i.e., if ABRs were used instead.

CONCLUSION

In summary, this report demonstrates the feasibility of recording acoustically evoked intracochlear potentials in an animal model. Our research is still evolving and we are currently working to implement soft electrodes and animals with hearing loss into our experimental setup. The present data also show our ability to detect robust potentials in response to acoustic stimuli and that we should be able to use a markedly abbreviated recording protocol which could then be used to obtain near real-time feedback. With further refinements, this recording paradigm could be combined with current cochlear implant technology. Specifically, all current FDA-approved cochlear implants have integrated recording features, which could be modified and used in conjunction with an acoustic stimulus generator.

Acknowledgments

REFERENCES

1. von Ilberg C, Kiefer J, Tillein J, et al. Electric-acoustic stimulation of the auditory system. New technology for severe hearing loss. ORL J Otorhinolaryngol Relat Spec. 1999; 61:334–340. [PubMed: 10545807]

2. Gstoettner WK, van de Heyning P, O'Connor AF, et al. Electric acoustic stimulation of the auditory system: results of a multi-centre investigation. Acta Otolaryngol. 2008; 128:968–975. [PubMed: 19086194]

3. Skarzynski H, Lorens A, Piotrowska A. A new method of partial deafness treatment. Med Sci Monit. 2003; 9:CS20–24. [PubMed: 12709676]

4. Simmons JA, Lavender WA, Lavender BA, et al. Target structure and echo spectral discrimination by echolocating bats. Science. 1974; 186:1130–1132. [PubMed: 4469702]

5. James C, Albegger K, Battmer R, et al. Preservation of residual hearing with cochlear implantation: how and why. Acta Otolaryngol. 2005; 125:481–491. [PubMed: 16092537]

6. Tyler RS, Gantz BJ, Rubinstein JT, et al. Three-month results with bilateral cochlear implants. Ear Hear. 2002; 23:80S–89S. [PubMed: 11883771]

7. Adunka OF, Pillsbury HC, Kiefer J. Combining perimodiolar electrode placement and atraumatic insertion properties in cochlear implantation -- fact or fantasy? Acta Otolaryngol. 2006; 126:475–482. [PubMed: 16698696]

8. Adunka O, Kiefer J, Unkelbach MH, Lehnert T, Gstoettner W. Development and evaluation of an improved cochlear implant electrode design for electric acoustic stimulation. Laryngoscope. 2004; 114:1237–1241. [PubMed: 15235353]

9. Adunka O, Gstoettner W, Hambek M, Unkelbach MH, Radeloff A, Kiefer J. Preservation of basal inner ear structures in cochlear implantation. ORL J Otorhinolaryngol Relat Spec. 2004; 66:306–312. [PubMed: 15668529]

10. Briggs RJ, Tykocinski M, Xu J, et al. Comparison of round window and cochleostomy approaches with a prototype hearing preservation electrode. Audiol Neurootol. 2006; 11(Suppl 1):42–48. [PubMed: 17063010]

11. Eshraghi AA, Polak M, He J, Telischi FF, Balkany TJ, Van De Water TR. Pattern of hearing loss in a rat model of cochlear implantation trauma. Otol Neurotol. 2005; 26:442–447. discussion 447. [PubMed: 15891647]

12. Eshraghi AA, Yang NW, Balkany TJ. Comparative study of cochlear damage with three perimodiolar electrode designs. Laryngoscope. 2003; 113:415–419. [PubMed: 12616189]

13. Adunka OF, Radeloff A, Gstoettner WK, Pillsbury HC, Buchman CA. Scala tympani cochleostomy II: topography and histology. Laryngoscope. 2007; 117:2195–2200. [PubMed: 17909447]

14. Briggs RJ, Tykocinski M, Stidham K, Roberson JB. Cochleostomy site: implications for electrode placement and hearing preservation. Acta Otolaryngol. 2005; 125:870–876. [PubMed: 16158535]

15. Skarzynski H, Fayette RP. A new cochlear implant electrode design for preservation of residual hearing: a temporal bone study. Acta Otolaryngol. 2009

16. Skinner MW, Holden TA, Whiting BR, et al. In vivo estimates of the position of advanced bionics electrode arrays in the human cochlea. Ann Otol Rhinol Laryngol Suppl. 2007; 197:2–24. [PubMed: 17542465]

17. Aschendorff A, Kromeier J, Klenzner T, Laszig R. Quality control after insertion of the nucleus contour and contour advance electrode in adults. Ear Hear. 2007; 28:75S–79S. [PubMed: 17496653]

18. Thorne M, Salt AN, DeMott JE, Henson MM, Henson OW Jr. Gewalt SL. Cochlear fluid space dimensions for six species derived from reconstructions of three-dimensional magnetic resonance images. Laryngoscope. 1999; 109:1661–1668. [PubMed: 10522939]

19. Rajan R, Irvine DR, Wise LZ, Heil P. Effect of unilateral partial cochlear lesions in adult cats on the representation of lesioned and unlesioned cochleas in primary auditory cortex. J Comp Neurol. 1993; 338:17–49. [PubMed: 8300898]

20. Saitoh I, Suga N. Long delay lines for ranging are created by inhibition in the inferior colliculus of the mustached bat. J Neurophysiol. 1995; 74:1–11. [PubMed: 7595762]

21. Robertson D, Irvine DR. Plasticity of frequency organization in auditory cortex of guinea pigs with partial unilateral deafness. J Comp Neurol. 1989; 282:456–471. [PubMed: 2715393]

22. Dallos P, Cheatham MA. Travel time in the cochlea and its determination from cochlear-microphonic data. J Acoust Soc Am. 1971; 49(Suppl 2):1140. + [PubMed: 5552191]

23. Dallos P, Schoeny ZG, Cheatham MA. On the limitations of cochlear-microphonic measurements. J Acoust Soc Am. 1971; 49(Suppl 2):1144. + [PubMed: 5552192]
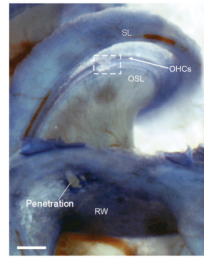
Figure 1.
Example of damage to basilar membrane caused by the electrode. The preparation shown is a decalcified toludine blue stained whole mount. Damage is outlined by the box. The physiology data in Figures 2-4 is from this case. SL: spiral ligament; OHCs: Outer hair cells; OSL: osseous spiral lamina; RW: Round window.
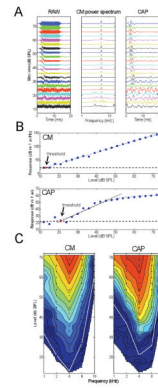
Figure 2.
Example CM and CAP recordings from just inside the round window. **A**: Level series at a single frequency (4 kHz). Left panel is the raw recording which contains the sinusoidal CM lasting for the duration of the stimulus and riding on the CAP which occurs near the beginning of the stimulus. Middle panel is the power spectrum of the CM, taken from an epoch (7-12 ms) uncontaminated by the CAP. Right panel is the raw recording filtered from 500-1.5 kHz to extract the CAP. Signals in each panel are normalized to the maximum amplitude for each stimulus level, such that the noise levels increase as the stimulus level is lowered. **B**: Thresholds for the CM and CAP were estimated as the stimulus level at which the response reached the noise floor. For the CM, the linear response was fit with a straight line. For the CAP, the saturating response was fit with a logistic function, and a line fit to slope at the 50% response magnitude. **C**: Contour plots of CM and CAP magnitude as a function of frequency and level. The color scale for the contour plot of the CM is from 25 (dark blue) to 160 dB (red, re 1 µV/Hz) and for the CM is from 25 to 60 dB (re 1 µV). The same color scales were used for all contour plots herein. Data points taken are shown as filled circles. The white lines are thresholds at each frequency.
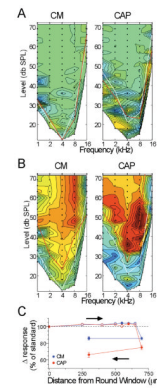
Figure 3.
Results of CM and CAP recordings at different depths of insertion. **A**: Depth = 250 mm. **B**: Depth=700 mm. These figures are contour plots of the difference between the standard response at the round window and the test response at the depth of insertion. Green is no difference, blue is an increased response and red is a decreased response compared to the standard (color scale of the CM is from 25, dark blue, to 160 dB, red, re 1 µV/Hz, and for the CM is from 25 to 60 dB, re 1 µV). White lines are the thresholds of the standard and red lines are the thresholds at the test depth. **C**: Results of the complete track in this case. Each point is the average response of all data points that were above threshold in either the test or standard, expressed as a percent of the average response level at the round window (responses measured in dB, as in Figure 2B).
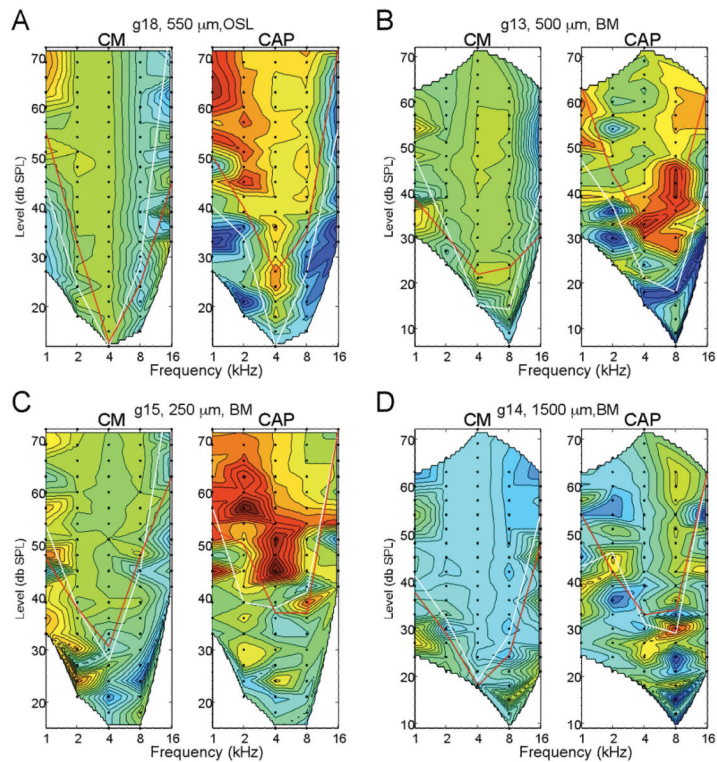
Figure 4.
Four examples where the CAP showed a loss of response where the CM did not. For each case, depth and site of anatomical damage is indicated. In each case the loss of response, indicated by warmer colors, in the CAP was significant while that of the CM was not. Note that in two cases (A and C), the loss of response occurred at low frequencies, while in two cases (B and D) it was primarily at high frequencies. This variability does not appear to be due to the site of damage, as changes in the same frequency ranges have been seen when the damage was to the BM or the OSL. The reverse scenario, on where the CM is reduced prior to the CAP, has not been seen in any animal tested so far. Thus, a slight decrease in the CAP response appears to be the most sensitive marker of cochlear damage under these conditions (color scale of the CM is from 25, dark blue, to 160 dB, red, re 1 µV/Hz, and for the CM is from 25 to 60 dB, re 1 µV).
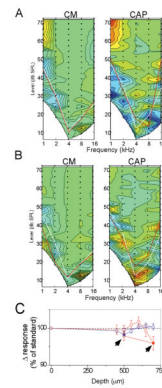
Figure 5.
Example of a case where the physiological changes were reversible when the electrode was withdrawn. **A**: An initial significant decrease in the CAP magnitude occurred at low frequencies and high intensities, with a smaller and not significant change in the CM. **B**: After the electrode was withdrawn, the response changes disappeared (color scale of the CM is from 25, dark blue, to 160 dB, red, re 1 µV/Hz, and for the CM is from 25 to 60 dB, re 1 µV). **C**: The complete track for this case, with the sites shown in A and B indicated by arrowheads (right arrowhead is shown in A, and left arrowhead is shown in B).
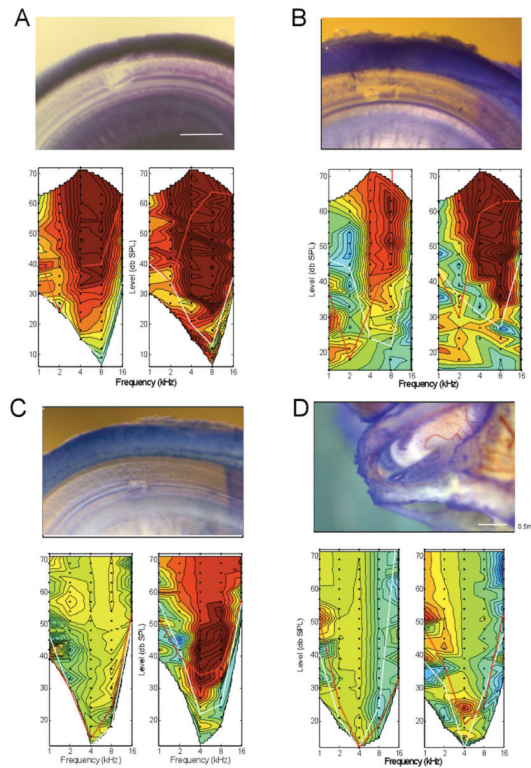
Figure 6.
A: Extensive damage on the basilar membrane; the loss of electrophysiologic activity was extensive and irreversible. The damage consisted of a clear breach of the basilar membrane, loss of hair cells, and damage to supporting cells lateral to the OHCs. **B**: Trauma similar to that previously seen in the case shown in Figures 1-4. The damage consisted of a clear breach of the basilar membrane, loss of hair cells and some supporting cells. The loss of response in the CAP was extensive but that to the CM was moderate. **C**: Damage on the basilar membrane restricted to a small site underneath the hair cells and tunnel of Corti. On close inspection there appeared to still be a thin layer of membrane separating the scala tympani and scala media. Although there was loss of hair cells, it is possible that the reticular lamina was either not breached such that mixing of endolymph and perilymph either did not occur or was minimal. The magnitude of response loss was moderate for the CAP, and minimal for the CM. **D**: No damage to the basilar membrane. Instead, there was a region of damage on the OSL, which appeared to be a flake of bone that was lifted up allowing stain to be trapped. In this case, the damage to both the CM and CAP was minimal, and reversed to a substantial degree after withdrawal of the electrode.

Table 1

Data on all 10 ears

Animal	Histology			Measurements at Round Window				Maximum Depth Traveled (mm)*	Frequency Range of Initial Damage		Depth First Damage Detected		Final Thresholds		Recovery after Retraction
	Ear	Site of Damage	Breach of Scala Media	CM CF (Hz)	CM Thresh. (dB SPL)	CAP CF (Hz)	CAP Thresh. (db SPL)		CM	CAP	CM (mm)*	CAP (mm)*	CM (db SPL)	CAP (db SPL)	
Gerbil #11	Right	OSL-BM	yes	8k	22	8k	27	1800	mid	high	1000	1000	48	>63	no
Gerbil #13	Right	BM	yes	8k	9	8k	13	1000	mid	high	750	500	51	>63	no
Gerbil #14	Left	BM	yes	4k	18	8k	15	1950	high	high	1700	1300	37	>63	no
Gerbil #15	Right	BM	yes	4k	23	4k	37	400	mid	low	400	250	>72	>72	no
Gerbil #18	Right	OSL	no	4k	16	4k	16	550	none	low	none	550	17	21	incomplete
Gerbil #21	Right	BM	yes	4k	13	4k	21	700	high	high	700	700	33	54	no
Gerbil #22	Right	None	no	4k	6	4k	15	700	none	low	none	650	6	9	complete
Gerbil #24	Right	BM	no	4k	12	4k	22	500	none	high	none	500	15	31	no
Gerbil #27	Right	BM	no	4k	11	4k	29	400	high	high	400	400	8	29	no
Gerbil #27	Left	OSL-BM	no	4k	13	4k	20	550	high	high	600	550	19	41	no

Abbreviations: **CM**: cochlear microphonics, **CAP**: compound action potential, **OSL**: osseous spiral lamina, **BM**: basilar membrane

*
all insertion depths were measured from the round window (via the micromanipulator)